HOSTED BY
ELSEVIER
Available online at www.sciencedirect.com
ScienceDirect
Soils and Foundations 59 (2019) 1160–1171
SOILS AND FOUNDATIONS
www.elsevier.com/locate/sandf

Technical Paper

Subsurface ground movements due to circular shaft construction

Binh Thanh Le [a,*], Richard James Goodey [b], Sam Divall [b]

[a] Faculty of Transportation Engineering, Ho Chi Minh City University of Transport, Viet Nam
[b] School of Mathematics, Computer Science & Engineering, Civil Engineering, City, University of London, London, UK

Received 1 February 2018; received in revised form 30 January 2019; accepted 20 March 2019
Available online 19 July 2019

Abstract

The rapid development of modern metropolises has led to a shortage of surface space and, in response, engineers have pursued alternatives below ground level. Shafts are commonly used to provide temporary access to the subsurface for tunnelling and, as permanent works, are utilised for lifts or ventilation purposes. The construction sequence of axisymmetric shafts makes them a dramatically simple solution. In addition, circular shafts are inherently stiffer than other plan geometries. Those are perhaps the reasons why circular shafts are preferred in situations of restricted space or unfavourable ground conditions. However, due to the lack of case histories reporting ground movements induced by shaft construction, no empirical prediction method for subsurface soil displacements exists. The work presented here seeks to provide clearer insights into surface and subsurface soil displacements induced by circular shaft construction by means of an analysis of measurements obtained from centrifuge tests and available field data. Novel empirical equations and procedures are then suggested for practical use.

Keywords: Shaft construction; Ground movements; Centrifuge modelling

1. Introduction

In urban environments, shafts are often, by necessity, constructed adjacent to existing underground structures such as tunnels, deep foundations and basements. This makes the understanding of subsurface ground deformations and how they relate to surface displacement profiles increasingly important in assessing the possible effects of the shaft excavation on nearby structures.

Faustin (2017) found that the magnitude and extent of ground deformations depend greatly on the shaft construction technique which can be classified into two categories: pre-installed shaft lining and concurrent shaft lining. In the former category, the shaft lining is installed before the shaft is excavated. The shaft lining can be formed by a precast lining, diaphragm wall or sheet piles. The concurrent shaft lining involves the excavation and then the construction of the shaft lining. In concurrent shaft lining methods, a spray-concrete lining (SCL) or precast segments are often used to form the lining.

The sources of ground deformations induced by shaft construction are depicted in Fig. 1 (after Faustin, 2017) and are described below:

(i) Radial unloading
- For the concurrent shaft lining: removing the soil causes stress relief that results in the movement of soil into the shaft cavity before the lining is installed.
- For the pre-installed shaft lining: when the soil within the lining is removed, the unbalanced horizontal stresses are transferred to the shaft lining resulting in lining compression, leading to horizontal and vertical soil displacements. As the soil is

Peer review under responsibility of The Japanese Geotechnical Society.
* Corresponding author.
E-mail address: binh.le@ut.edu.vn (B.T. Le).

https://doi.org/10.1016/j.sandf.2019.03.013

Nomenclature

List of symbols

a	constant indicates the depth at which maximum horizontal displacement occurs
b	constant governs the height of the Gaussian curve
d	distance from shaft wall
D	shaft diameter
H	shaft depth
K_0	ratio between horizontal and vertical effective stresses at rest
OCR	overconsolidation ratio
n	multiple of shaft depth H to distance d from the shaft wall where settlement becomes zero
S	soil displacement
S_v	vertical soil displacement
S_h	horizontal soil displacement
S_v^{dz}	vertical displacement at depth z and at distance d from shaft wall
S_h^{dz}	horizontal displacement at depth z and at distance d from shaft wall
S_u	undrained shear strength of clay
α	empirical constant
$\varnothing_c'$	critical state angle of shearing resistance
σ_h'	horizontal effective stress
σ_v'	vertical effective stress
σ_{v0}	maximum consolidation pressure for clay model in centrifuge test

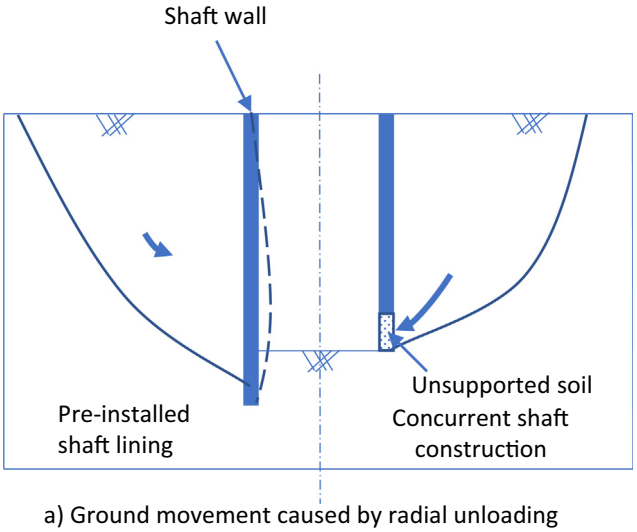

Fig. 1. Sources of ground movements due to shaft construction (after Faustin, 2017).

supported by the shaft lining, the magnitude of the soil displacements is expected to be smaller than that in the concurrent shaft construction where the horizontal stress is reduced to zero without support prior to the installation of the shaft lining. This was confirmed by a back analysis of the field data reported by Faustin (2017).

(ii) Vertical unloading of the excavated base causes heave at the shaft plug which also contributes to the total soil deformation.

(iii) Changes in the ground water table due to dewatering causes settlement. However, dewatering is not necessarily performed in all cases.

(iv) Consolidation due to the changes in pore water pressure in the ground re-establishes equilibrium as a result of the excavation process. In the available case histories, only Schwamb (2014) reported long-term settlements which were considered minor compared with those which occurred during diaphragm wall construction. Due to this lack of reliable long-term data, the current work only reports and analyses short-term soil displacements due to a shaft excavation and does not consider long-term movements due to either consolidation or creep.

Up to 2016, there were only a few empirical approaches for surface settlement $S_v^{surface}$ prediction including the widely used equation suggested by New and Bowers (1994).

$$S_v^{surface} = \alpha H \left(1 - \frac{d}{H}\right)^2 \quad (1)$$

It is important to note that Eq. (1) was derived from field measurements from only one shaft with $H = 26m$ and $D = 11$ m, constructed using the concurrent shaft sinking technique in London Clay. The prediction of

surface settlements using this equation would be dependent on the adopted value of α. In the original work, the reported value of $\alpha = 6 \times 10^{-4}$ provided the best fit with the field data presented in New and Bowers (1994), but the literature does not contain any further reported values (Schwamb et al., 2016). Eq. (1) is acknowledged to be quite conservative, particularly for pre-installed shafts (Schwamb, 2014; Faustin, 2017) because, for those conditions, the settlements are expected to be smaller, as was discussed earlier.

New (2017) studied field data from 13 shaft construction projects, with a diameter range of $D = 6.5$ to 16.6 m, and found that the magnitude of the surface settlement increases with a larger shaft diameter (Fig. 2). An extension to New and Bowers (1994) original equation was suggested by New (2017); it introduces a new variable, n, which governs that the surface settlement becomes zero at a distance of nH from the shaft wall, as described in Eq. (2).

$$S_v^{surface} = \alpha H \left(1 - \frac{d}{nH}\right)^2 \tag{2}$$

The field measurements presented by New (2017) are all from projects in stiff London Clay with a similar construction technique. As such, the original value of α was retained in this work, but the values of n and α would be expected to increase in softer soils. New (2017) suggested that designers can consider Eq. (2) as a predictive tool with the values of n and α to be chosen dependent on the required degree of conservatism and that they should be supported by field data from similar shaft projects. New (2017) also acknowledged that surface settlement predictions are varied and difficult to make due to a lack of available field data. Whilst this work enables designers to assess surface settlements, there is no empirical approach for predicting subsurface soil displacements even though more shafts are being constructed in crowded and sensitive urban areas with existing buried structures. These structures may require an assessment of the effect of adjacent shaft construction in order that their serviceability be maintained.

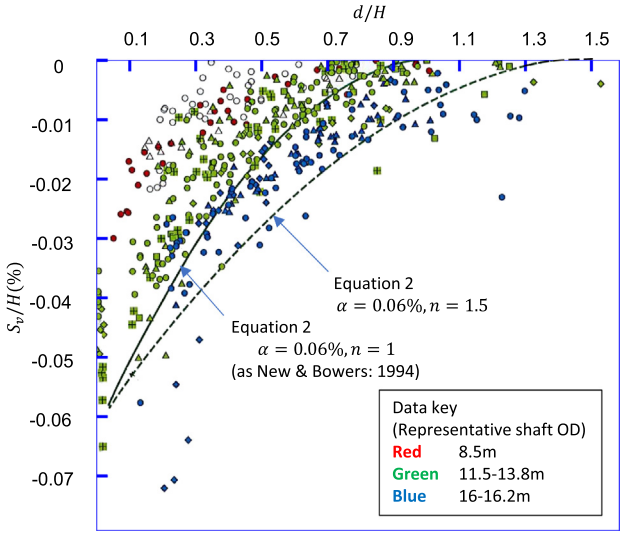

Fig. 2. Surface settlement data from 13 shafts (after New, 2017).

The main purpose of the study presented in this paper is to gain a better insight into subsurface soil displacements induced by shaft construction by means of centrifuge modelling and a back analysis of available case histories.

2. Case studies

An extensive literature review on shaft construction, carried out by Faustin (2017), shows that there were only 18 case histories of circular shaft construction published between 1980 and 2016. There were some additional cases in 2017 (Faustin, 2017; New, 2017). Most of these case studies reported surface settlement, only three cases presented subsurface soil displacements and only one case reported surface horizontal displacement. Details of the case histories used in this section are presented in Table 1 with shaft geometries, construction techniques and soil conditions.

It is worth noting that not all measurements from these publications are reported in this paper. Even though there were data from four extensometers in Schwamb et al. (2016), the readings from two of them were less than 0.5 mm which is well below the resolution of the instrumentation, and therefore, they are not presented here. Hence, only the readings from two extensometers in Wong and Kaiser (1988) and Schwamb et al. (2016) are used for the subsurface vertical displacement analysis.

Only one of the two inclinometer measurements reported by McNamara et al. (2008) and Wong and Kaiser (1988) are also utilised in this study. This is because the other inclinometer readings were either affected by existing piles (McNamara et al., 2008) or were not fully reported, possibly due to poor accuracy (Wong and Kaiser, 1988).

Even though there were two data sets for horizontal and vertical surface displacements available in New and Bowers (1994), only one set was used because the other was deemed unreliable due to the effects of heavy plant movements and nearby excavations.

The rarity of high quality field measurements from shaft construction in the literature is possibly due to the high cost of monitoring schemes especially for deep shaft construction where deep drilling, for casings to house inclinometers and extensometers, is required to be below the shaft plug level in order to achieve representative results. In addition, shaft construction sites are normally occupied with activities that may affect the measurements, leading to unrepresentative data, and the existence of underground structures may alter the soil deformation mechanisms which causes difficulties in interpreting the measurement results.

The challenges in obtaining representative soil displacements due to shaft construction can be overcome by the centrifuge modelling technique due to its advantageous

Table 1
Case histories used in this paper.

No	Reference	Location	Construction method	Ground conditions	Shaft geometry		Available ground movements data
					D (m)	H (m)	
1	Wong and Kaiser (1988)	Edmonton, Canada	Concurrent shaft lining Corrugated and Flanged steel plates	Sand & clay (6.5 m) Glacial matrix (13 m) Clay shale	2.4–3.2	20	Surface: Sv Subsurface Sh, Sv
2	Schwamb et al. (2016)	London, UK	Pre-installed shaft lining Diaphragm wall	London basin deposits	30	73	Subsurface Sh, Sv
3	McNamara et al. (2008)	London, UK	Concurrent shaft lining Pre-cast segments	London clay (30 m) Lambeth Group (18 m)	8.2	37.5	Subsurface Sh
4	New and Bowers (1994)	London, UK	Concurrent shaft lining Pre-cast segments (16 m) SCL (10 m)	Superfical deposits (3.5 m) London Clay	10.65	26	Surface Sh, Sv
5	This study	City, University of London	Pre-installed shaft lining	Speswhite kaolin	8*	20*	Surface Sv, Sh Subsurface Sv, Sh

* Dimension in equivalent prototype.

capabilities in modelling the soil behaviour in geotechnical events (Taylor, 1995). Recent developments in technology allow for the accurate measurement of soil deformations at any position in small-scale centrifuge models (Stanier et al., 2015; Le et al., 2016).

3. Centrifuge testing

A bespoke centrifuge model (Fig. 3) was designed and used to investigate soil deformations induced by shaft construction and is described here.

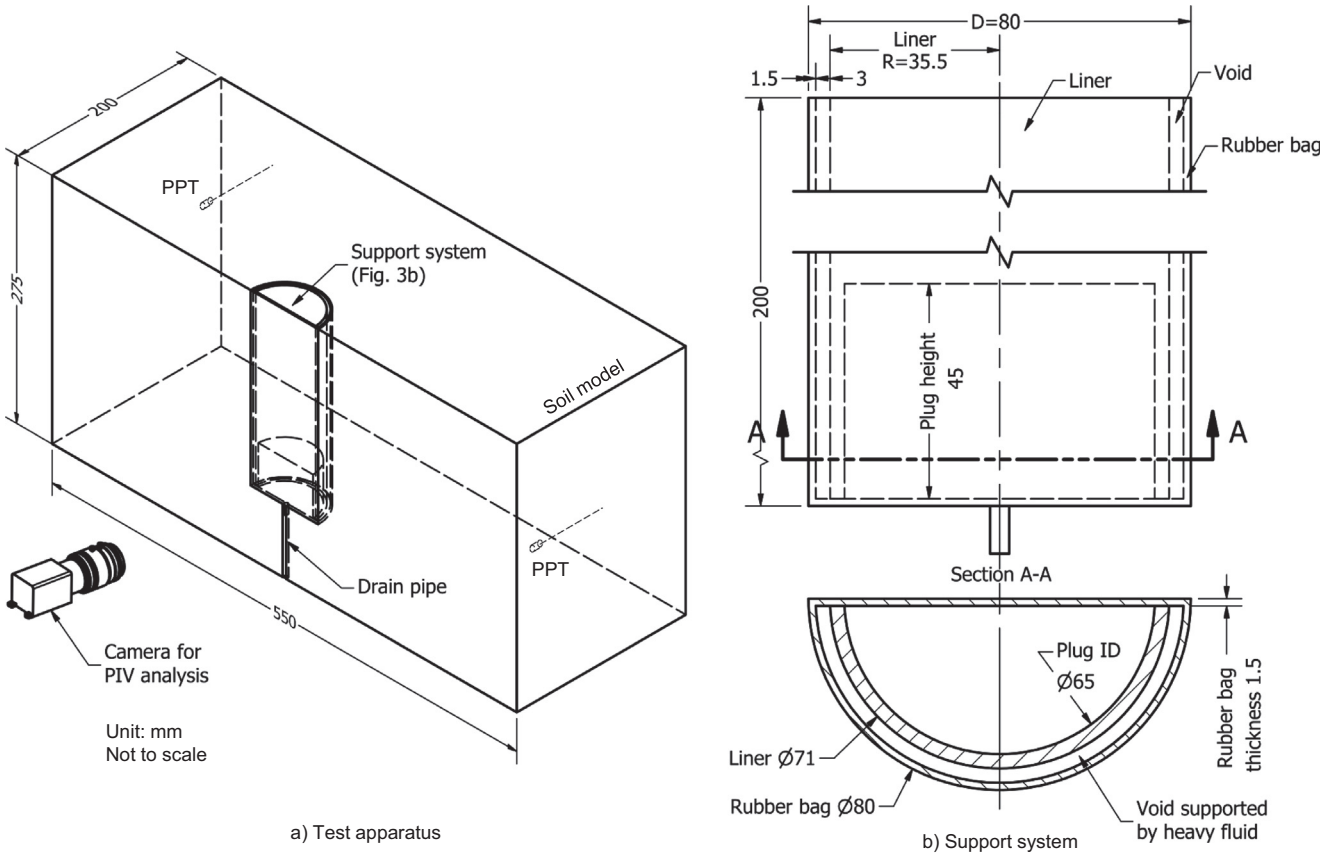

Fig. 3. Schematic of centrifuge test apparatus.

3.1. Test series

The tests were performed using a fixed geometry, but varying the undrained shear strength S_u of the clay. The clay model (Speswhite kaolin) was consolidated one dimensionally in a soil container (known as a strong box) using a hydraulic consolidometer to a maximum vertical effective stress σ'_{v0} equal to 350 kPa and 500 kPa for test CR350 and CR500, respectively. The samples were swelled back to a vertical stress of 250 kPa for both tests. The consolidation pressures were chosen for the following three reasons:

- To achieve overconsolidated soil, representative of the real soil in urban environments (Parry, 1970);
- For the clay to be stiff enough for model making;
- For the clay not to be so stiff that the soil deformations, induced by the simulated shaft excavation, would not be too small to measure accurately.

The water table was set at the soil surface level. Properties of the Speswhite kaolin used here can be found in Grant (1998). More details on the testing apparatus and the procedure can be found in Divall and Goodey (2016) and are described briefly below.

3.2. Test apparatus

A schematic of the centrifuge model is illustrated in Fig. 3. The excavation was simulated by a semi-circular cavity cut into the clay which could be viewed through the front Perspex window of the centrifuge model container. The dimensions of the excavation are $D = 80$ mm and $H = 200$ mm. The excavation is supported by two components:

- The shaft liner (Fig. 3b): 200 mm high and 71 mm in diameter. The cavity in the shaft plug (Fig. 3b) has an internal diameter of 65 mm and a depth of 45 mm to allow basal heave to develop during the excavation simulation.
- A latex bag encloses the shaft liner with the cavity filled with a heavy fluid (commercially known as Sodium Polytungstate or SPT). This SPT fluid was prepared to have a density equal to the clay used in the model, 17.5 kN/m^3, in order to provide support to the soil.

The latex bag has a thickness of 1.5 mm and, together with the liner with a radius of R equal to 35.5 mm, leaves a void of 3 mm between the excavation and the liner. This is initially supported by the heavy fluid of which the head was set to be level with the ground surface. The excavation process was simulated by draining the heavy fluid to generate radial and vertical unloading that results in ground deformations including heaving at the bottom of the shaft.

It is worth noting that using heavy fluid to support the soil implies an assumption that $K_0 = 1$, i.e., $\sigma'_v = \sigma'_h$, within the soil mass, which is slightly different from the K_0 calculated by Eq. (3) (Mayne and Kullhawy, 1982) and shown in Fig. 4.

$$K_0 = \left(1 - sin\varnothing'_c\right) OCR^{sin\varnothing'_c} \tag{3}$$

For Speswhite kaolin, $\varnothing'_c = 23^\circ$ (Grant, 1998). It can be seen that the K_0 values calculated by Eq. (3) for the soil along the shaft depth (0–200 mm) are close to 1 (Fig. 4). Near the surface, the values of K_0 are much larger. However, as the vertical stresses near the surface are very small, the effect of this dissimilarity in K_0 is negligible and was confirmed by the good agreement between the centrifuge test results and the field measurements which are presented later in this paper.

3.3. Test procedure

On the test day, the strong box was removed from the hydraulic consolidometer to begin the model-making procedure. All exposed surfaces of the clay sample were sealed with silicone oil to prevent drying and, from this point onwards, the model-making process was carried out as rapidly as possible in order to preserve the stress history of the soil. The clay was then trimmed to the correct model height, and a semi-circular cavity was cut so that the shaft support system could be placed within it. The front face of the clay model was sprayed with dyed Leighton Buzzard Sand (Fraction B) to create the texture necessary for optimising the geoPIV post-test analysis. The front Perspex window was then bolted to the model container before the heavy fluid was injected into the rubber bag.

The models were accelerated to 100 g and left running until the clay had reached effective stress equilibrium. The excavation process was then simulated by draining

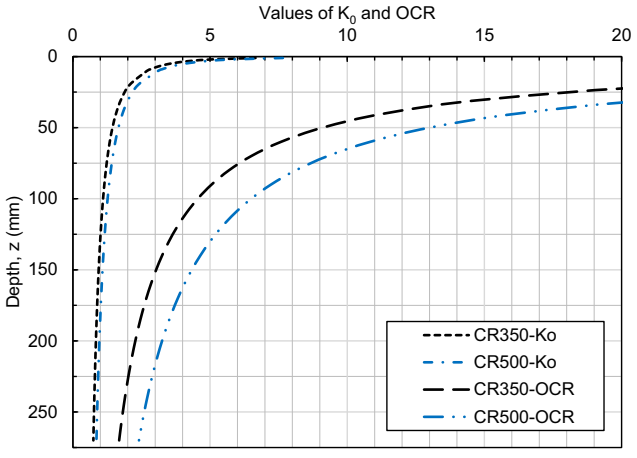

Fig. 4. Profiles of K_0 and OCR with depth in centrifuge models.

the heavy fluid. Data related to the deformations of the clay model and the heavy fluid level were recorded at 1-second intervals for later analysis. In practice, the unloading rate varies in different projects due to different soil conditions, shaft geometries and construction techniques. Therefore, the construction rate for these centrifuge tests was selected to ensure an undrained response to unloading. The total time required to simulate the complete unloading event was 25 s in the centrifuge which represents around 2.5 days at the prototype scale. The model was then spun down and shear vane readings were carried out to determine the undrained shear strength, S_u, of the clay model.

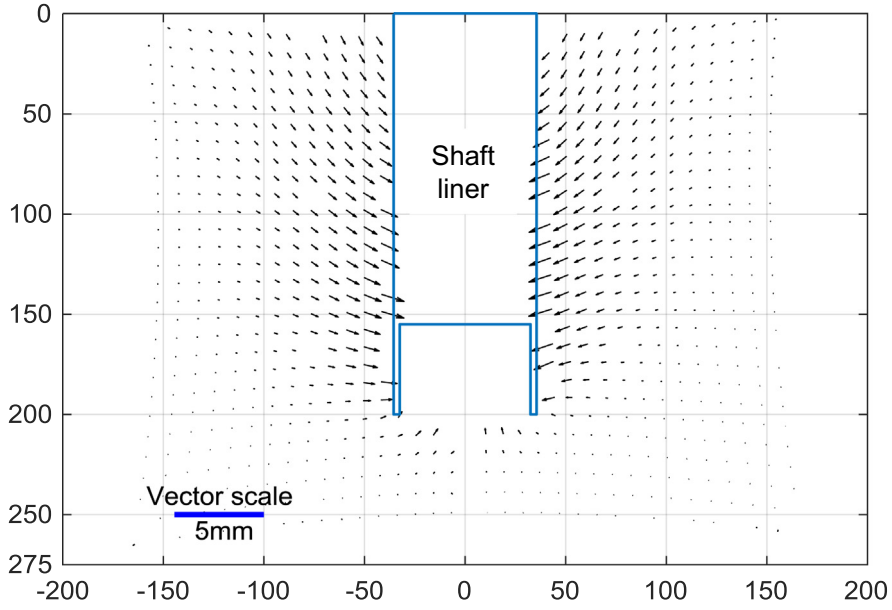

a) Soil displacement field

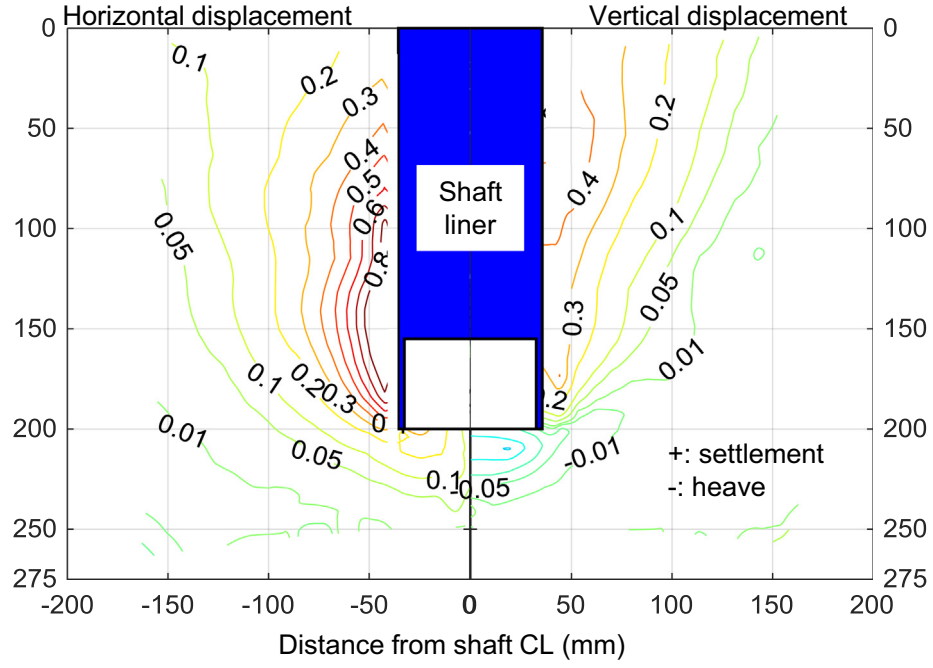

b) Horizontal and vertical displacement contours

Fig. 5. Soil deformations in test CR500 after all fluid was drained out.

The average S_u of the model clay from the surface to the shaft plug were 44.5 kPa and 57.8 kPa for tests CR350 and CR500, respectively.

3.4. Measurement of soil movements

GeoPIV_RG (Stanier et al., 2015) was used to analyse the soil movements at the front face of the model from the digital images taken during the test (Fig. 3a). One of the drawbacks of using a digital image analysis in centrifuge modelling is the friction at the interface between the Perspex window and the soil model that may affect the soil movement mechanism. However, the results from the image analysis reported by Grant (1998), Divall (2013) and Le (2017) showed that once the soil at the interface moved, it continued to displace at the same rate as the rest of the model. Therefore, the friction at the interface is negligible to the development of soil displacements and their mechanisms. Le (2017) conducted a series of shear box tests to examine the friction at the interface and found that the texture material was the key factor. In this research, Leighton Buzzard Sand was used as it induced less friction compared with other texture materials (e.g. glass balotini) owing to its lower angle of friction.

4. Test results

The typical soil displacements immediately after all the fluid was drained out of the rubber bag, in centrifuge test CR500, are presented in Fig. 5a, and the corresponding displacement contours are presented in Fig. 5b. It can be seen that the soil displacements are symmetrical (Fig. 5a). From Fig. 5b, soil displacements in the vertical and horizontal directions become very small (less than 0.01 mm) at a distance of 150–200 mm from the shaft centreline. This confirms that the soil container was large enough and the boundary effects were negligible.

Fig. 6 illustrates the vertical and horizontal soil displacements in test CR500 at various distances up to 80 mm ($0.4H$) away from the shaft wall. For clarity, only the data on one side of the model are presented. The vertical displacement increases towards the shaft wall and decreases with depth which is similar to observations made by previous researchers (New and Bowers, 1994; New, 2017; Faustin, 2017; Schwamb et al., 2016). Interestingly, the profile of displacements S_h and S_v, with depth z, at various distances from the shaft wall (up to $d = 40$ mm $= 0.2H$), shows similar distribution patterns. For data at a distance beyond 40 mm from the shaft wall, for example, $d = 80$ mm (Fig. 6), the distribution of the displacements with depth shows a different shape. Further analysis of the subsurface and the surface soil displacements is discussed below.

4.1. Subsurface soil vertical displacements

Fig. 7 presents subsurface vertical movement profiles at various distances $d = 0.05H$ to $0.2H$ from the shaft wall at the end of the two centrifuge tests along with data from Wong and Kaiser (1988) and Schwamb et al. (2016). The

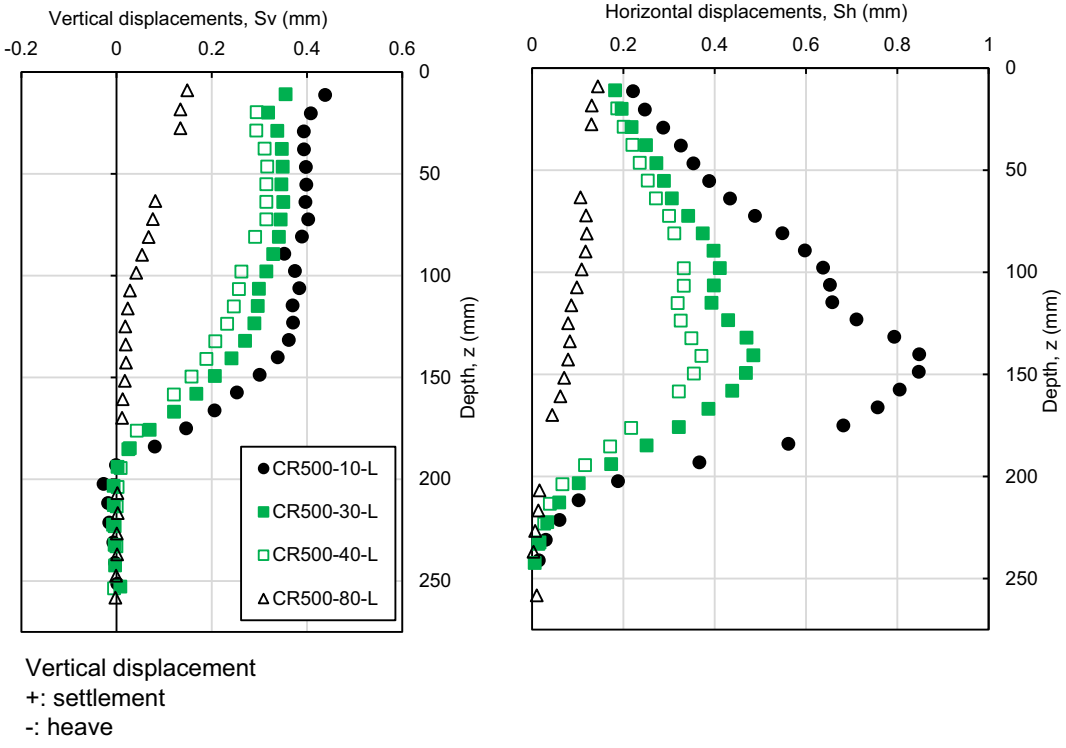

Fig. 6. Typical subsurface soil displacements in test CR500.

vertical movement at depth z and a distance d from the wall, S_v^{dz}, is normalised by the maximum settlement at that distance, S_{vmax}^{d}, and z is normalised by H. The results from both centrifuge tests fit well with the data from Wong and Kaiser (1988), but not with the data from Schwamb et al. (2016); the likely reason is explained below.

In Schwamb et al. (2016), the extensometer readings were baselined with bottom anchors which were installed at depths higher than that of the base of the shaft. The extensometer readings can only reflect absolute movements if the bottom anchors are fixed. However, the finite element analysis showed that the removal of the overburden pressure at the excavation surface caused the adjacent ground to heave and the bottom anchor of the rod extensometers to move upwards by approximately 3 mm (Schwamb et al., 2016). The heave behaviour near the shaft plug is confirmed by the centrifuge tests (Figs. 5–7). If the extensometer data are corrected by adding 3 mm to the readings, then the profile of the subsurface vertical movements from Schwamb et al. (2016) (labelled as corrected) is also in good agreement with the other data (Fig. 7). It is worth noting that the bottom extensometer in Wong and Kaiser (1988) was installed into the clay shale layer, presumably a very stable stratum, and below the shaft plug level.

Despite the differences in soil conditions, construction techniques and excavation dimensions in the considered shafts, vertical movements at depth z, S_v^z, when plotted in the manner of Fig. 7, show a consistent distribution which can be described by Eq. (4):

$$\frac{S_v^{dz}}{S_{vmax}^{d}} = 1.15 - \frac{0.15}{1 - z/H} \tag{4}$$

(applicable for $z \leq 0.9H$)

Eq. (4) and Fig. 7 show that the maximum vertical movement occurs near the ground surface (when $z = 0$) and decreases with depth.

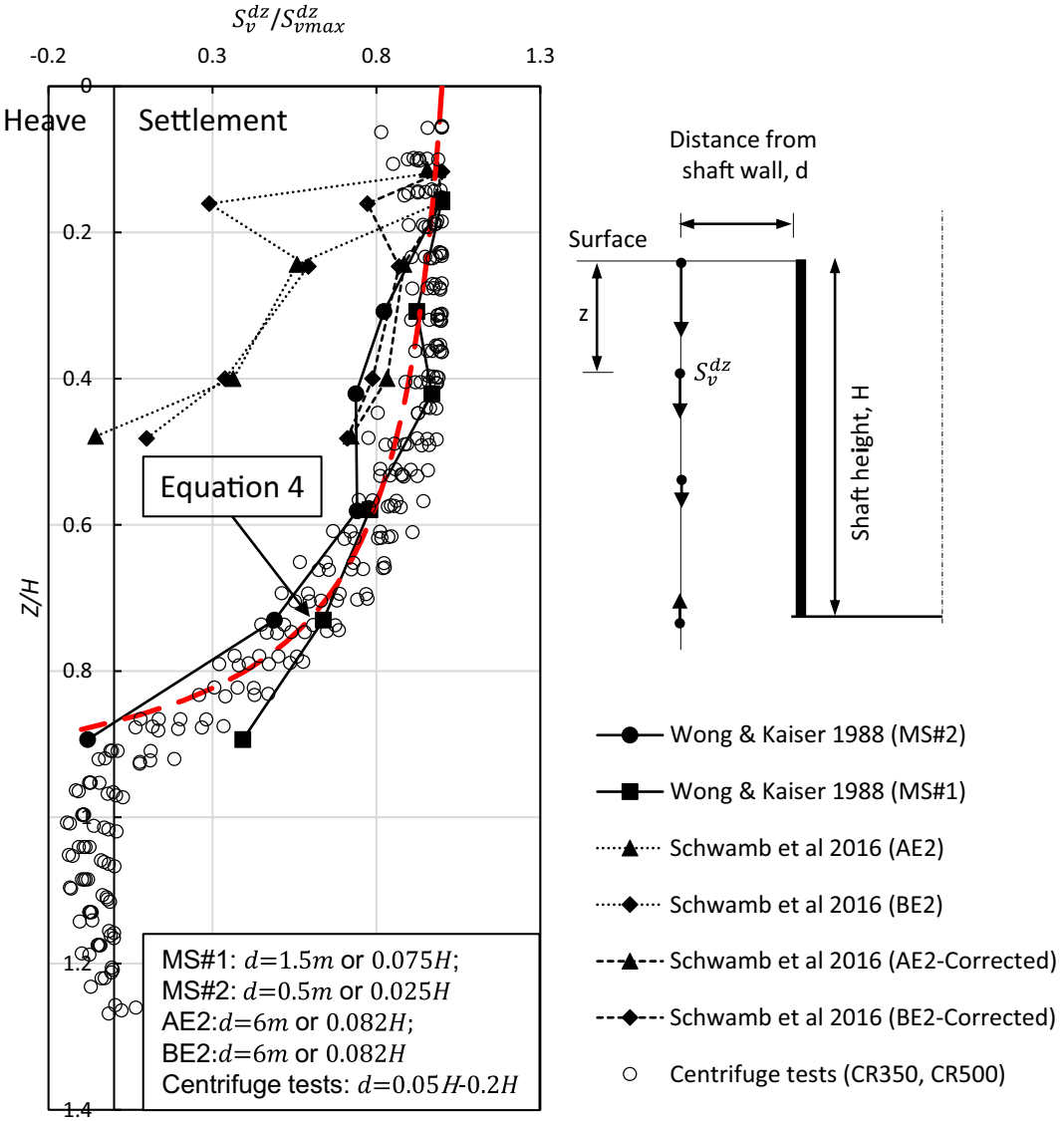

Fig. 7. Subsurface vertical movements.

4.2. Subsurface soil horizontal displacements

Fig. 8 presents the subsurface horizontal soil movements in the considered shafts, reported by McNamara et al. (2008) and Wong and Kaiser (1988), together with the results from two centrifuge tests. Horizontal movement at depth z and at a distance d from the wall, S_h^{dz}, is normalised against the maximum horizontal displacement at that radial distance, S_{hmax}^{d} and depth z is normalised against H. Despite there being some anomalies from the field measurements, most of the data points agree well with the trend shown by the centrifuge test results.

The profile of horizontal soil movements with depth shows a similar distribution to a Gaussian curve with the maximum value at $z/H = 0.6$ to 0.8. This is thought to be analogous to the horizontal load distribution against a retaining wall where the load acts at depth $z/H = 2/3 \approx 0.67$. A best fit Gaussian curve (Eq. (5)) is proposed and also plotted in Fig. 8.

$$\frac{S_h^{dz}}{S_{hmax}^{d}} = \exp\left[-\left(\frac{z/H - a}{b}\right)^2\right] \tag{5}$$

where $a = 0.6$ implies that S_{hmax}^{d} occurs at $z = 0.6H$; $b = 0.4$ governs the height of the Gaussian curve.

The values of a and b can be varied to find a best fit Gaussian curve.

New (2017) commented that there is inadequate field data for a reliable prediction of the horizontal soil

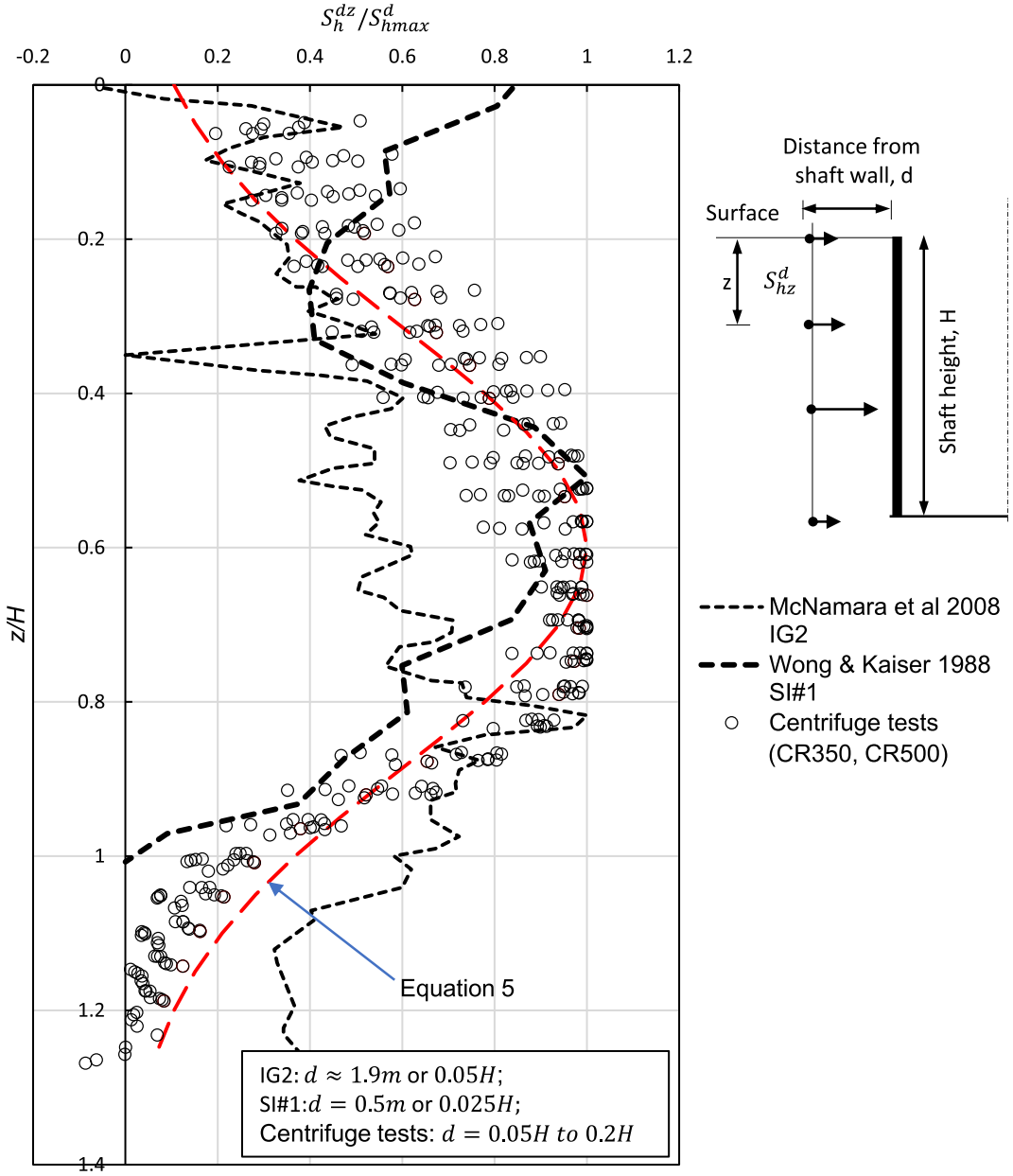

Fig. 8. Subsurface horizontal movements.

displacements and that these are normally assumed to have a similar magnitude to the vertical soil displacements. Similarly, GCG (2007) suggested that for ground movements due to shaft excavation at the surface, $S_{hmax}^{surface} = S_{vmax}^{surface}$. In order to examine this assumption, Fig. 9 plots the vertical and horizontal displacements at the surface from test CR500 and the field measurements from New and Bowers (1994). Again, for clarity, only the data from one side of test CR500 are presented along with the field measurements. Whilst the data plotted in Fig. 9 are not directly comparable (due to significantly large differences in undrained shear strength), it is clear from both the centrifuge test results and the field measurements that the maximum surface vertical displacement is significantly larger than the maximum horizontal displacement. Therefore, the assumption of $S_{hmax}^{surface} = S_{vmax}^{surface}$ may lead to the overestimation of the horizontal displacement, especially at the subsurface as S_{hz} increases with depth z, as shown in Fig. 8.

Most of the centrifuge test data (with $d < 0.2H$), some of which is presented in Fig. 6, show values of $S_{hmax}^{d}/S_{vmax}^{d}$ in the range 1 to 1.9. As shown in Fig. 7 and Eq. (4), the maximum settlement occurs at surface $S_{vmax}^{d} = S_{v}^{d-Surface}$. With a surface settlement profile estimated by Eq. (2), assuming $S_{hmax}^{d} = (1 \text{ to } 1.9)S_{v}^{d-surface}$ allows for a range in horizontal displacements at a distance d at any depth z to be estimated using Eq. (5) (which would ideally be supported by similar case studies). The data from Fig. 9 show the soil displacements in the vertical and horizontal directions to be considerably smaller in the field compared with those measured in the centrifuge. New and Bowers (1994) reported values of S_u in London Clay varying from 50 kPa to 250 kPa, whereas those in centrifuge test CR500 had an average S_u of approximately 58 kPa. Given the information related to the undrained shear strengths of clay in the centrifuge tests and the literature contained in this paper, engineers can make judgements based upon the specific site soil conditions when estimating soil displacements. The assumption $S_{hmax}^{d} = (1 \text{ to } 1.9)S_{v}^{d-surface}$ is examined in a back analysis on field measurements later in this paper.

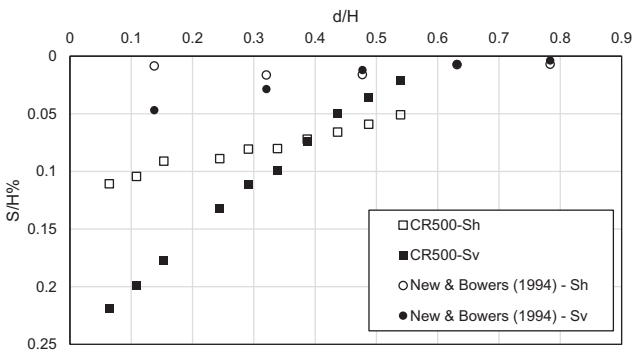

Fig. 9. Displacements at surface in centrifuge test and New and Bowers (1994).

5. Comparison between centrifuge tests and shaft excavation in practice

There are clearly significant differences between the reported experiments and the construction of a shaft in practice. These differences are primarily related to the method and the rate of construction as well as to the stiffness of the shaft lining. As previously stated, the rate of unloading in the tests was chosen in order to replicate, as much as possible, an undrained event. The field data utilised here comes from a variety of projects in a variety of soil conditions which may or may not behave in an undrained way. Nevertheless, a good agreement between this field data and the centrifuge tests has been reported which suggests that the unloading rate had a negligible impact on the soil displacements during the shaft excavation.

When considering the shaft lining, it could be assumed that the relative hoop stiffness will have an effect on the magnitude of the soil displacements around the shaft excavation (a fact also noted by Schwamb et al., 2016). The focus of the current work is the pattern, rather than the magnitude, of the subsurface soil displacements induced by shaft excavations. From Figs. 7 and 8, it can be seen that despite the (assumed) difference in relative hoop stiffness of the shafts in the reported case histories compared with the centrifuge tests (arising from the use of different shaft linings and construction methods), the patterns of the subsurface soil displacements were observed to be similar. This implies that relative hoop stiffness has a negligible impact on the patterns of the subsurface soil displacements induced by the shaft excavation.

6. Example application of new equations

Fig. 10 presents a flow chart on how to use Eqs. (2), (4) and (5) to predict subsurface vertical and horizontal displacements. The data set from Wong and Kaiser (1988) is used to demonstrate their applicability.

The first stage of the prediction is to generate suitable values of n and α for use in Eq. (2). As previously stated,

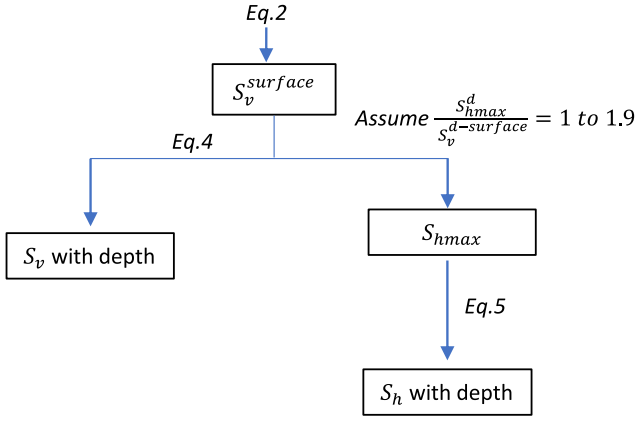

Fig. 10. Suggested flow chart on usage of proposed equations.

New (2017) acknowledged that these values should be selected with reference to similar case histories; however, in this example, no such data are available. As such, the original values of New (2017) are adjusted by assessing the ground conditions and the geometry of the shaft reported by Wong and Kaiser (1988). The shaft diameter of Wong and Kaiser (1988) is approximately four times smaller than that in the cases reported in New (2017), and the undrained strength of the soils is estimated to be 50% of the strength of London Clay. A narrower shaft is likely to lead to a narrowing of the surface settlement extent (i.e., a reduction in n) and a decrease in the generated settlements (i.e. a reduction in α). The decrease in soil strength is likely to lead to an inverse effect (i.e. an increase in settlements and the extent reflected by increases in n and α). Using this rationale, estimates of n and α are derived from the original values of $n = 1.5$ and $\alpha = 6 \times 10^{-4}$ by doubling these values (to account for the decrease in soil strength) and then reducing them by a factor of 4 (to account for the decrease in shaft diameter). This leads to an overall factor of 0.5, and thus, values of $n = 0.75$ and $\alpha = 3 \times 10^{-4}$.

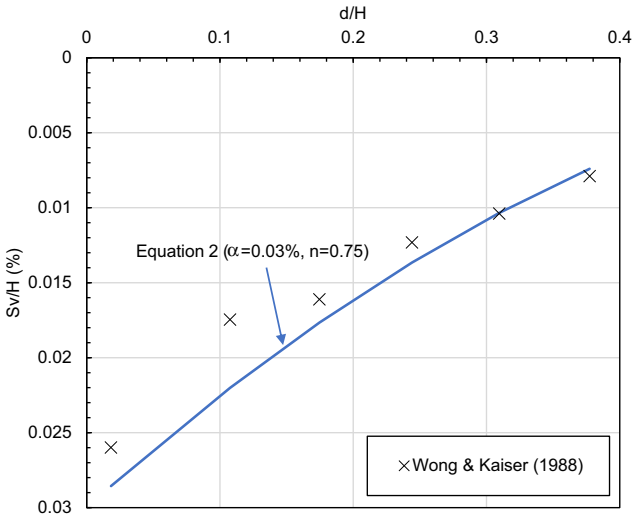

Fig. 11. Comparison of surface settlement in Wong and Kaiser (1988) and back analysis using Eq. (2).

Using these values in Eq. (2) leads to the profile of the surface settlement shown in Fig. 11. Also plotted in this figure are the data from Wong and Kaiser (1988) which show a reasonable agreement with the profile generated by Eq. (2), whilst acknowledging that the basis for the selection of the n and α values is open to interpretation. A best fit exercise to the measured data was carried out resulting in very good agreement between the data and Eq. (2). The values of n and α arising from this exercise were 0.85 and 2.55×10^{-4}, respectively. However, for the purposes of this discussion, the original estimated values are used.

The surface settlements at the positions of inclinometer SI#1 ($d = 0.5$ m) and extensometer MS#1 ($d = 1.5$ m) are determined as $S_{v-surface}^{SI\#1} = 5.61$ mm and $S_{v-surface}^{MS\#1} =$

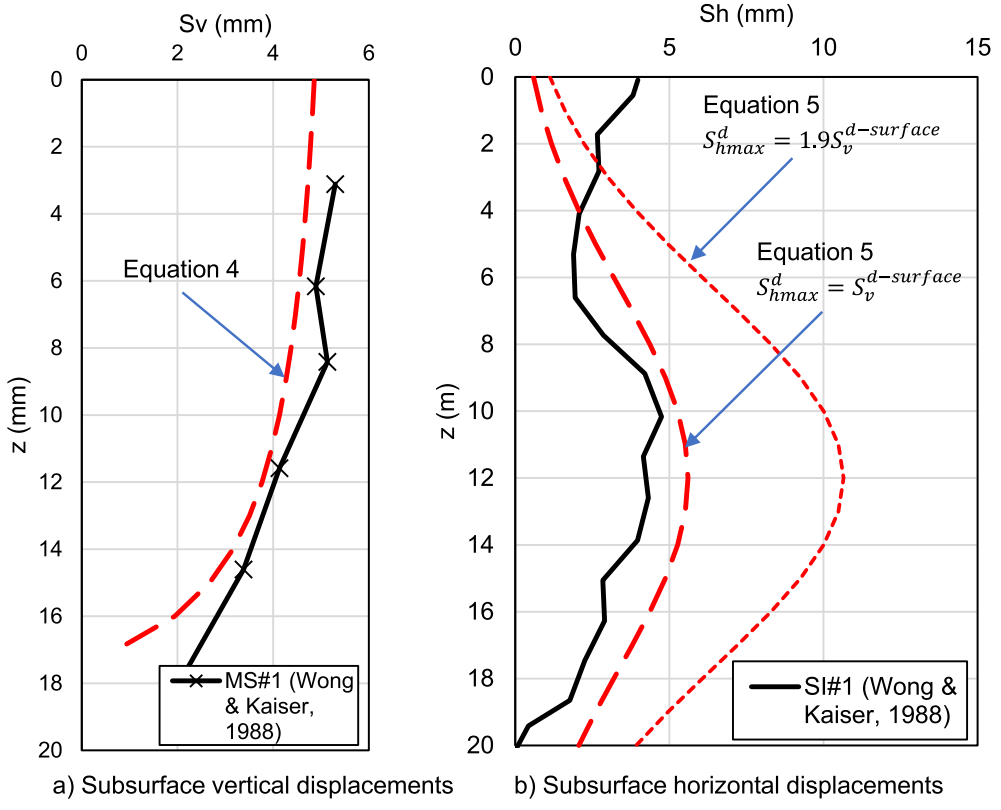

Fig. 12. Comparison of subsurface soil displacements in Wong and Kaiser (1988) and back analysis using Eqs. (4) & (5).

4.86 mm, respectively, using distance d in Eq. (2). Thus, Eqs. (4) & (5) with the determined $S_{v0}^{MS\#1}$ and $S_{hmax}^{SI\#1}$ give subsurface vertical and horizontal displacements which are plotted in Fig. 12a & b along with the corresponding field measurements. The limits of the range identified from the centrifuge tests, $S_{hmax}^{d}/S_{v}^{d-surface} = (1 \text{ to } 1.9)$, are used to generate the two curves in Fig. 12b.

The predicted vertical displacement with depth is marginally smaller than the measured value. Nevertheless, the predicted vertical displacement with depth is very similar to the field measurement in terms of magnitude and shape.

For subsurface horizontal displacement, the assumption of $S_{hmax}^{d} = S_{v}^{d-surface}$ provided a very good fit with the field measurement, whereas $S_{hmax}^{d} = 1.9S_{v}^{d-surface}$ overestimated the magnitude of the soil deformations. More field data are needed to assess whether $S_{hmax}^{d} = S(1 \text{ to } 1.9)_{v}^{d-surface}$ and caution should be exercised when applying this relationship.

7. Conclusion

The results of the centrifuge tests carried out in this research show a good agreement with the field data from various shaft projects which provides a clearer insight into subsurface soil displacements due to shaft excavation. Based on the experimental evidence and the field measurements, two novel empirical equations have been suggested to describe the unique distributions of soil movements with depth regardless of the soil conditions, the construction techniques and the shaft dimensions. A flow chart on how to use these equations to predict soil movements in any direction and at any point has been provided for practical use.

Acknowledgements

The authors gratefully acknowledge the support of the Leverhulme Trust (Grant no. RPG-2013-85) and the support from colleagues at the Research Centre for Multi-scale Geotechnical Engineering, at City, University of London.

References

Divall, S., 2013. Ground movements associated with twin-tunnel construction in clay, PhD thesis. University of London, City.

Divall, S., Goodey, R.J., 2016. An apparatus for centrifuge modelling of a shaft construction in clay. In: Eurofuge2016, 3rd European Conf. on Physical Modelling in Geotechnics, Nantes, France.

Faustin, N.E., 2017. Performance of circular shafts and ground behaviour during construction PhD thesis. University of Cambridge.

GCG, 2007. Settlement Estimation Procedure: Box Excavations & Shafts. B London, Crossrail. Report number: 1D0101-G0G00-01004.

Grant, R.J., 1998. Movements around a tunnel in two-layer ground PhD thesis. City, University of London.

Le, B., 2017. The effect of forepole reinforcement on tunnelling-induced movements in clay PhD thesis. University of London, City.

Le, B.T., Nadimi, S., Goodey, R.J., Taylor, R.N., 2016. System to measure three dimensional movements in physical models. Géotech. Lett. 6 (4), 256–262.

Mayne, P.W., Kulhawy, F.H., 1982. Ko-OCR relationships in soil. J. Soil Mech. Found. Div. 108 (6), 851–872.

McNamara, A., Roberts, T., Morrison, P., Holmes, G., 2008. Construction of a deep shaft for Crossrail. In: Proc. Instn Civ. Engrs Geotech. Engng, vol. 161, pp. 299–309.

New, B., 2017. Settlements due to shaft construction. In: Tunnels and Tunnelling International, September 2017, pp. 16–17.

New, B., Bowers, K., 1994. Ground movement model validation at the Heathrow Express trial tunnel. Tunnelling '94 Proc. 7th Int. Symp. IMM and BTS. Chapman and Hall, London, pp. 301–329.

Parry, R.H.G., 1970. Overconsolidation in soft clay deposits. Géotechnique 20 (4), 442–446.

Schwamb, T., 2014. Performance Monitoring and Numerical Modelling of a Deep Circular Excavation. Phd thesis. University of Cambridge.

Schwamb, T., Soga, K., Elshafie, M.Z.E.B., Mair, R.J., 2016. Considerations for monitoring of deep circular excavations. Proc. Instn Civ. Engrs Geotech. Eng. 169 (6), 477–493.

Stanier, S.A., Blaber, J., Take, W.A., White, D.J., 2015. Improved image based deformation measurement for geotechnical applications. Can. Geotech. J.

Taylor, R.N. (Ed.), 1995. Geotechnical Centrifuge Technology. Blackie Academic and Professional, Glasgow.

Wong, R.C.K.R., Kaiser, P.P.K., 1988. Behaviour of vertical shafts: reevaluation of model test results and evaluation of field measurements. Can. Geotech. J. 25 (2), 338–352.